

Interaction between Viruses and Clays in Static and Dynamic Batch Systems

VASILIKI I. SYNGOUNA AND
CONSTANTINOS V. CHRYSIKOPOULOS*

Department of Civil Engineering, Environmental Engineering
Laboratory, University of Patras, 26500 Patras, Greece

Received January 12, 2010. Revised manuscript received
April 28, 2010. Accepted May 10, 2010.

Bacteriophage MS2 and Φ X174 were used as surrogates for human viruses in order to investigate the interaction between viruses and clay particles. The selected phyllosilicate clays were kaolinite and bentonite (>90% montmorillonite). A series of static and dynamic experiments were conducted at two different temperatures (4 and 25 °C) to investigate the effect of temperature and agitation (dynamic experiments) on virus adsorption onto clays. Appropriate adsorption isotherms were determined. Electrokinetic features of bacteriophages and clays were quantified at different pH and ionic strength (IS). Moreover, interaction energies between viruses and clays were calculated for the experimental conditions (pH 7 and IS = 2 mM) by applying the DLVO theory. The experimental results shown that virus adsorption increases linearly with suspended virus concentration. The observed distribution coefficient (K_d) was higher for MS2 than Φ X174. The observed K_d values were higher for the dynamic than static experiments, and increased with temperature. The results of this study provided basic information for the effectiveness of clays to remove viruses by adsorption from dilute aqueous solutions. No previous study has explored the combined effect of temperature and agitation on virus adsorption onto clays.

Introduction

Viruses in natural waters and wastewaters are frequently found attached onto sand, clays, bacterial cells, naturally occurring suspended colloids, sludge particles, and estuarine silts and sediments (1, 2). The survival and persistence of viruses adsorbed onto clays in natural habitats is greater than that of suspended viruses (3–6). The mechanisms associated with virus adsorption onto clays are not well understood, and different viruses appear to have different affinities for various clays (7, 8).

Viral adsorption onto mineral surfaces is primarily controlled by electrostatic surface charge (9, 10), hydrophobicity (11, 12), and water chemistry (10, 13). Very few studies have quantified the electrokinetic features of bacteriophages at different pH and IS (12, 14). Electrokinetic measurements may be influenced by the aggregation state of the viral suspension (15, 16). However, electrokinetic properties of viruses are not fully understood (17–19).

The surface charge heterogeneities of clay minerals influence particle interactions in clay mineral suspensions (20–22), which can affect colloid, biocolloid, and contami-

nant sorption. Although many researchers have investigated the electrokinetic properties of clay minerals (23, 24) and have examined the sorption of bacteriophages and pathogenic viruses onto clays and other minerals (8, 9, 11, 19, 25, 26), the interaction between viruses and clays is not fully understood.

In this work, batch experiments were conducted to investigate virus sorption onto various clay minerals at two different temperatures under static and dynamic conditions. To our knowledge, no previous study has investigated the combined effect of temperature and agitation on virus adsorption onto clays. The surface properties of viruses and clays were evaluated by electrophoretic mobility measurements over a large range of pH and IS. To explore the interactions between viruses and mineral surfaces, Derjaguin–Landau–Verwey–Overbeek (DLVO) potential energy profiles were constructed for the experimental conditions by modeling viruses as colloidal particles and using measured zeta potentials.

Materials and Methods

Bacteriophage MS2 and Φ X174 were used in this study as surrogates for human viruses. MS2 is a F-specific, single-stranded RNA phage with 31% nucleic acid content, whose host bacterium is *E. coli* ATTC 15597-B1; whereas, Φ X174 is an icosahedral, single-stranded DNA phage with 26% nucleic acid content, whose host bacterium is *E. coli* ATTC 13706-B1. The MS2 particle diameter ranges from 24 to 26 nm, whereas, the Φ X174 particle diameter ranges from 25 to 27 nm. MS2 has hydrophobic protein coat, whereas Φ X174 has hydrophilic protein coat (27). The preparation of stock and purification of bacteriophages were made according to the ATCC procedure as described by Adams (28). Both bacteriophages were assayed by the double-layer overlay method (28), where 0.1 mL of the appropriate host bacterium and 0.1 mL of diluted virus sample solution were mixed in a centrifuge tube. The mixture was combined with molten soft-agar medium (4.5 mL) maintained at 45 °C in a tube and poured onto a Petri dish containing solid agar medium. The plates were solidified for 10 min and incubated overnight at 37 °C. Viable virus concentrations were determined by counting the number of plaques in each host lawn and reported as plaque-forming units per milliliter (PFU/mL). Only dilutions that resulted in the range of 20–300 plaques per plate were accepted for quantification. All virus concentrations reported represent the average of two replicate plates.

The clays used in this investigation were the crystalline aluminosilicates: kaolinite (03584 Kaolinite, Fluka, chemical composition: Al_2O_3 ~37.6%, SiO_2 ~47.3%, Fe_2O_3 ~0.5%, TiO_2 ~0.4%, K_2O ~1.8%, Na_2O ~0.1%, loss on calcination ~12%) and bentonite (18609 Bentonite, Riedel de Haen, > 90% montmorillonite, chemical composition: SiO_2 59.2%, Al_2O_3 18.5%, Fe_2O_3 5.6%, CaO 2.0%, MgO 4.0%, Na_2O 0.2%, K_2O 0.9%, weight loss on ignition 8.7%). The principal building elements of the clay minerals are two-dimensional arrays of silicon–oxygen tetrahedra (tetrahedral silica sheet) and that of aluminum- or magnesium-oxygen-hydroxyl octahedra (octahedral, alumina, or magnesia sheet). The sharing of oxygen atoms between silica and alumina sheets results in two-layer minerals (TO) or three-layer minerals (TOT) (20, 29). Kaolinite is a two-layer or TO clay, whereas montmorillonite, the predominant clay mineral in bentonite, is a three-layer or TOT clay. Montmorillonite has the ability to absorb water molecules in the interlayer surfaces of the clay lattice. Also, montmorillonite has a higher cation exchange capacity than

* Corresponding author phone: +30 2610 996531; fax: +30 2610 996573; e-mail: gios@upatras.gr.

kaolinite. Furthermore, the two minerals differ in their BET specific surface area, which is defined as the external surface area per unit of mass (kaolinite: $\sim 9 \text{ m}^2/\text{g}$, bentonite: $\sim 80 \text{ m}^2/\text{g}$, as measured by the manufacturer). The $< 2 \mu\text{m}$ colloid fractions of the clays used for hydrodynamic diameter and zeta potential measurements were obtained by stirring 0.5 g of clay within 50 mL deionized (DI) water for a 12-h period at pH 7. The solution was allowed to rest for a 24 h period before an aliquot from the supernatant was taken for measurements (30).

The sorption behavior of MS2 and ΦX174 onto kaolinite and bentonite was characterized at two different controlled temperatures (4 and 25 °C), under static and dynamic batch conditions. Control tubes, in the absence of clay, were used to monitor virus inactivation due to factors other than adsorption to clays (e.g., inactivation or sorption onto the tube walls). The batch equilibration method used consists of adding a virus stock solution into a 50 mL glass centrifuge tube containing 0.5 g of the clay at a concentration of 10 mg clay per mL of PBS solution (solids to solution ratio: 1 to 100). Glass tubes were used in order to minimize virus inactivation (31, 32). Different virus stock concentrations ranging from 10^3 to 10^9 PFU/mL were used. Each concentration was diluted from the same virus stock solution with a low IS phosphate-buffered saline (PBS) solution at pH 7, as suggested by various investigators (32–35). The PBS solution was prepared with 1.2 mM NaCl, 0.027 mM KCl, and 0.010 mM phosphate buffer salts in UV-disinfected distilled water with a specific conductance of $17.8 \mu\text{S}/\text{cm}$. The specific conductance of the final virus suspension was $212 \mu\text{S}/\text{cm}$, which corresponds to $\text{IS} \approx 2 \text{ mM}$. The control tubes were treated in the same fashion as the reactor tubes. Only for the dynamic batch experiments the reactor and control tubes were attached to a small benchtop tube rotator. For both static and dynamic batch experiments, samples were collected every 24 h for a period of 7 days and centrifuged at 2000g (6000 rpm) for 30 min in a Cole Palmer mini microcentrifuge. This 7 day time-period was determined to be sufficient for the bacteriophage-clay systems to reach equilibrium. Other studies focusing on bacteriophage sorption onto soil suggest that virus concentrations in control tubes are consistently lower than in reactor tubes (36).

A zetasizer (Nano ZS90, Malvern Instruments, Southborough, MA) was used to measure the zeta potential and hydrodynamic diameter of bacteriophage and clay particles in PBS solution at pH 7 and $\text{IS} = 2 \text{ mM}$ at 25 °C in order to ensure that adsorption experiments were performed with monodispersed viruses. All zeta potential and hydrodynamic diameter measurements were obtained in triplicates.

For the quantification of the electrokinetic features (zeta potential) of bacteriophage and clay particles over a broad IS range (1–200 mM), the background electrolyte used was KCl because PBS was shown to cause aggregation. Viral aggregation in PBS has also been observed in other studies (14, 15), and is known to influence electrokinetic measurements (15, 16). Furthermore, the isoelectric point (IEP), the pH where the electrophoretic mobility changes from positive to negative, of MS2, ΦX174 , and clay particles was determined by diluting bacteriophage stocks and clay colloids in DI water and varying the pH from 2.5 to 11 with 0.1 M HNO_3 and 0.1 M NaOH. Note that the IEP measurements were obtained in DI water because the pH_{IEP} for MS2 stored in PBS is lower than that for MS2 stored in DI water (14), probably due to binding of phosphate to lysine on MS2 surfaces, which leads to positively charged sites.

Theoretical Calculations

The time dependent concentration of viruses sorbed onto a clay, C^* (PFU/mg clay), was calculated by (31):

$$C^*(t) = \frac{C_0(t) - C(t)}{M} \quad (1)$$

where C_0 (PFU/mL) is the suspended virus concentration at time t in the control tube, C (PFU/mL) is the suspended virus concentration at time t in the reactor tubes with a clay, and M (mg clay/mL) is the mass of clay added per volume of virus suspension. Note that inactivation rates for suspended and adsorbed viruses may be different (37–41). However, preliminary results have shown that under the experimental conditions of this study the virus inactivation rates in the control and reactor tubes are quite similar.

The zeta potential represents the electric potential difference between the interfacial double layer at the location of the slipping plane and the bulk fluid away from the interface, and customarily is denoted by the Greek letter zeta (ζ). The zeta potential is measured with a zetasizer instrument, which converts the measured electrophoretic mobility, U_E , (the velocity of a particle divided by the magnitude of the electric field) to zeta potential by using the Smoluchowski equation (42):

$$\zeta = \frac{4\pi\mu}{\epsilon} U_E \quad (2)$$

where μ is the dynamic viscosity of the suspending liquid, and ϵ is the dielectric constant of the suspending liquid.

The surface potentials, Ψ , of bacteriophages and clays are determined using measured zeta potentials ($\zeta < 60 \text{ mV}$) as follows (43):

$$\Psi = \zeta \left(1 + \frac{z}{r_p} \right) e^{\kappa z} \quad (3)$$

where $z \approx 3$ to 5 \AA is the distance between the charged particle surface and its slipping plane, r_p (\AA) is the Stokes or hydrodynamic radius of particles, and κ ($1/\text{m}$) is the inverse Debye–Hückel length, which is given by (44):

$$\kappa = \left[\frac{2I_s N_A 1000 e^2}{\epsilon \epsilon_0 k_B T} \right]^{-1/2} \quad (4)$$

where I_s (mol/L) is the ionic strength, N_A ($1/\text{mol}$) is Avogadro's number, e (C) is the elementary charge, k_B (J/K) is the Boltzmann constant, and T (K) is the temperature.

The intersurface potential energy equals the sum of the van der Waals, Φ_{vdW} , double layer, Φ_{dl} , and Born, Φ_{Born} , potential energies over the separation distance, x (m), between the approaching surfaces (25):

$$\Phi_{\text{tot}}(x) = \Phi_{\text{vdW}}(x) + \Phi_{\text{dl}}(x) + \Phi_{\text{Born}}(x) \quad (5)$$

The Φ_{vdW} (J) for sphere-plate interactions was calculated with the following expression (45):

$$\Phi_{\text{vdW}}(x) = -\frac{A_{123} r_v}{6x} \left[1 + \left(\frac{14x}{\lambda} \right) \right]^{-1} \quad (6)$$

where A_{123} (J) is the complex Hamaker constant, and $\lambda \approx 10^{-7} \text{ m}$ is the characteristic wavelength of the sphere-plate interaction. This expression is quite accurate for short distances (up to 20% of the particle radius). The complex Hamaker constant for the interacting media (bacteriophage–water–clay) was set to $A_{123} = 7.5 \times 10^{-21} \text{ J}$ (46) for both ΦX174 -mineral and MS2-mineral water systems. The Φ_{dl} for sphere-plate geometry was calculated with the expression (47):

$$\Phi_{dl}(x) = \pi \epsilon \epsilon_0 r_v \left[2 \Psi_v \Psi_c \ln \left(\frac{1 + e^{-\kappa x}}{1 - e^{-\kappa x}} \right) + (\Psi_v^2 + \Psi_c^2) \ln(1 - e^{-2\kappa x}) \right] \quad (7)$$

where ϵ_0 [$C^2/(J \cdot m)$] is the permittivity of free space, r_v (m) is the radius of the virus, Ψ_v (V) is the surface potential of the virus, and Ψ_c (V) is the surface potential of the clay. Note that eq 7 is valid for surface potentials <60 mV. The Φ_{Born} (J) was formulated as (44):

$$\Phi_{Born}(x) = \frac{A_{123}\sigma^6}{7560} \left[\frac{8r_v + x}{(2r_v + x)^7} + \frac{6r_v - x}{x^7} \right] \quad (8)$$

where σ (m) is the Born collision parameter. For the commonly used value of $\sigma = 5 \text{ \AA}$ (44), the resulting acceptable minimum separation distance is estimated to be $x \approx 2.5 \text{ \AA}$, which compares well to $x = 4\text{--}10 \text{ \AA}$ estimated by other investigators (48, 49). Note that Φ_{Born} can easily be neglected if $x > 1 \text{ nm}$.

Results and Discussion

For each deposition kinetics experiment one equilibrium adsorption value was obtained. The equilibrium adsorption data from the static and dynamic experiments of virus adsorption onto kaolinite and bentonite at two different temperatures are shown in Figure 1 for $\Phi X174$ and Figure 2 for MS2. The equilibrium adsorption data were fitted well with a linear isotherm:

$$C^* = K_d C_{eq} \quad (9)$$

where C_{eq} (PFU/mL) the virus concentration at equilibrium, and K_d (mL/mg sorbent) is the distribution coefficient.

Figures 1 and 2 indicate that for most of the cases examined the adsorption of both $\Phi X174$ and MS2 increase with increasing temperature, except for static experiments with $\Phi X174$ -bentonite and MS2-kaolinite, and it is higher for dynamic than static conditions except for $\Phi X174$ -kaolinite at 25 °C. Due to the agitation, the number of accessible sites for attachment is much higher in dynamic than static experiments. Agitation improves the contact of particles with the liquid and decreases the resistance to mass transfer (50). Therefore, attachment rates are lower for static conditions. This finding has also been observed in previous studies (51). Generally, hydrophobic interactions are more stable at higher temperatures (52). Furthermore, if sorption is controlled by partitioning of the hydrophobic part of a bacteriophage onto a clay particle, the sorption process is expected to increase with temperature (53). The experimental data suggest that, with the exception of kaolinite at 25 °C in static experiments, the adsorption onto both clays is greater for MS2 than $\Phi X174$, which is attributed to the higher hydrophobicity of MS2. Furthermore, virus adsorption was higher onto bentonite than kaolinite for both MS2 and $\Phi X174$, with the only exception of $\Phi X174$ onto kaolinite at 25 °C. Note that the bacteriophages and clays employed in this study were negatively charged at pH 7 of the experiments. Although, bacteriophage adsorption onto clays is often attributed to the large surface area and high cation exchange capacity of clays (35), in this study it is not trivial to correlate the observed virus adsorption with clay properties. However, it has been reported in the literature that virus adsorption onto clay minerals and organic particulates occurs either by physical means, as a result of van der Waals forces and hydrogen bonding (54), or through the formation of a cation bridge between net negatively charged viruses and net negatively charged clay minerals (55). The mechanisms and sites of

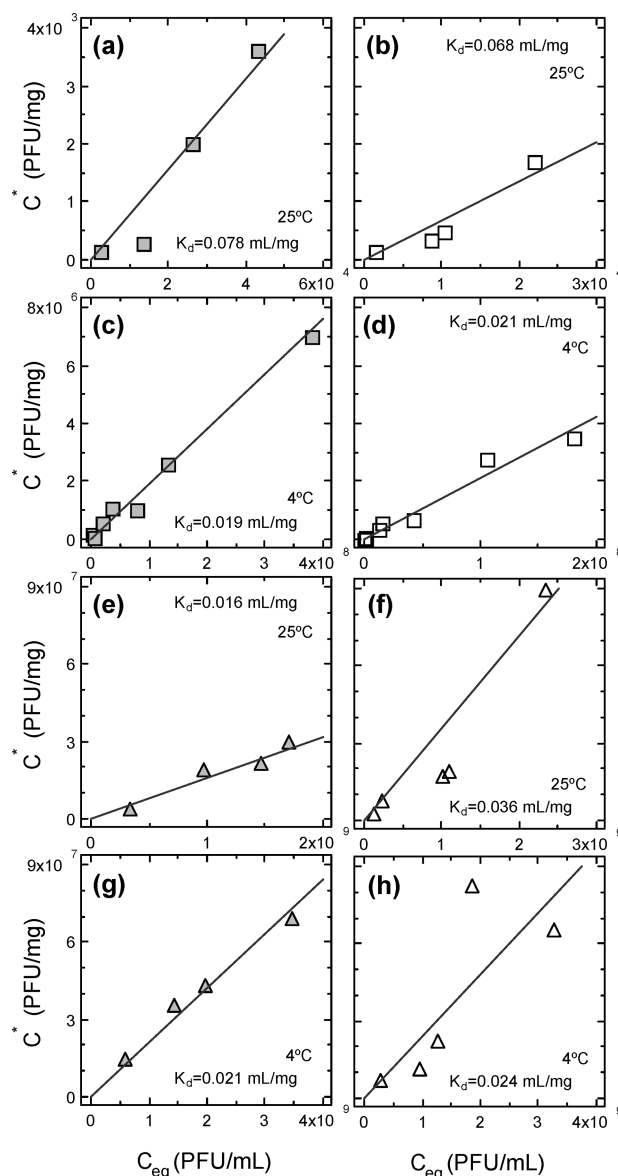


FIGURE 1. Equilibrium adsorption data (isotherms) at two different temperatures of $\Phi X174$ onto (a, b, c, d) kaolinite and (e, f, g, h) bentonite. The solid symbols indicate static and open symbols dynamic conditions. Squares represent kaolinite and triangles bentonite. The solid lines are fitted lines with slope equal to K_d and R^2 in the range 0.615–0.989.

sorption differ for different viruses and are influenced by the anion and cation exchange capacity of the clays (7).

The zeta potential of MS2, $\Phi X174$, kaolinite, and bentonite stored in PBS solution (pH 7, IS = 2 mM) were determined to be -40.4 ± 3.7 , -31.78 ± 1.25 – -49.5 ± 0.75 , and -29.5 ± 0.8 mV, respectively. MS2 stored in PBS solution was aggregated because its measured hydrodynamic radius was $r_v = 80.35$ nm, which is much greater than the radius of an individual MS2 particle (~ 12 nm). At pH 6.0, phosphate is expected to bind to positively charged lysine, an amino acid residue found on MS2 surfaces (56), and link MS2 particles together to form aggregates up to 300–400 nm (14). Also, $\Phi X174$ stored in PBS solution was aggregated because its measured hydrodynamic radius was $r_v = 151.3$ nm, which is much greater than the radius of an individual $\Phi X174$ particle (~ 13 nm). Aggregation of MS2 and $\Phi X174$ has also been observed by other investigators (12). To avoid the possibility of biased zetasizer measurements, the use of

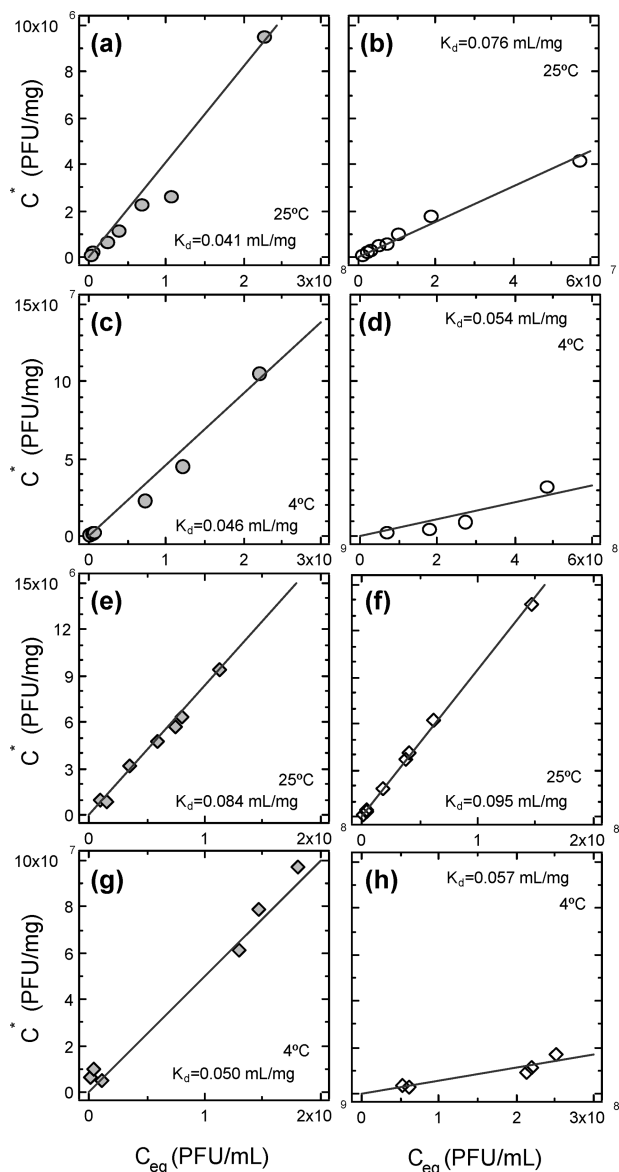


FIGURE 2. Equilibrium adsorption data (isotherms) at two different temperatures of MS2 onto: (a, b, c, d) kaolinite, and (e, f, g, h) bentonite. The solid symbols indicate static and open symbols dynamic conditions. Circles represent kaolinite and diamonds bentonite. The solid lines are fitted lines with slope equal to K_d and R^2 in the range 0.812–0.999.

another method for verification of virus aggregates is recommended.

The average particle size of kaolinite and bentonite at pH 7 was measured to be $r_c = 350$ and 400 nm, respectively. Note that for $\text{pH} < 4$, clay particles aggregate because their face and edge surfaces are oppositely charged, favoring the formation of agglomerates (57).

The influence of IS on bacteriophage and clay zeta potentials is presented in Figure 3a. For IS in the range 0.001 – 0.2 M at pH 7, the zeta potential of all surfaces is negative. The zeta potential, for all surfaces except bentonite, becomes less negative with increasing IS due to compression of the electrostatic double layer and screening of surface charge (58). The zeta potential of bentonite particles does not change significantly with IS. Figure 3b shows that the zeta potential of both kaolinite and bentonite particles suspended in DI water were negative over the pH range examined. Kaolinite is more sensitive to pH changes than bentonite. These findings are consistent with those reported

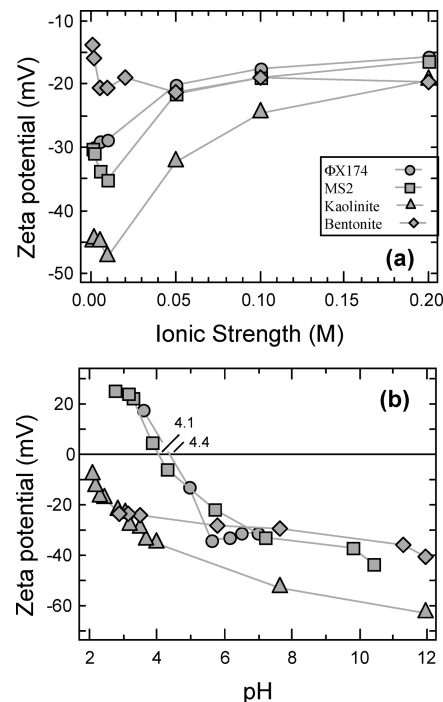


FIGURE 3. Zeta potential of ΦX174 , MS2, kaolinite, and bentonite, measured in DI water as a function of (a) IS, and (b) pH. The predicted pH_{IEP} values for ΦX174 and MS2 are 4.1 and 4.4, respectively.

by others (57, 59). The observed minor effect of IS and pH on zeta potential for kaolinite is attributed to the cation exchanges that occur at internal cation exchange sites in montmorillonite, which leave most of the external pH dependent sites unaffected. The IEP of MS2 and ΦX174 in DI water were found $\text{pH}_{\text{IEP}} 4.1$ and 4.4 , respectively. The IEP for MS2 stored in PBS ($\text{pH}_{\text{IEP}} 2.2$) is lower than MS2 stored in DI water ($\text{pH}_{\text{IEP}} 3.3$), probably due to binding of phosphate to lysine on MS2 surfaces, which creates phosphate-covered positively charged sites (14). Note that the results in Figure 3b are based on suspensions in DI water, and they may be somewhat different for other solutions. Nonetheless, our experimental IEP value for MS2 compare well with reported values of $\text{pH}_{\text{IEP}} 3.5$ (16, 60, 61), and 3.8 (19). Also, our experimental IEP value for ΦX174 is within the range of reported values $\text{pH}_{\text{IEP}} 2.6$ (12) to 6.6 (62). A feasible explanation of this discrepancy could be the possibly different IS and ΦX174 subpopulations. Also, the zeta potential concept was developed for hard particles. Consequently, zeta potential values derived from measured U_E values using the Smoluchowski equation (eq 2) may not accurately represent the surface potential of bacteriophages (16).

Figure 4 illustrates the total potential interaction energy curves, according to DLVO theory, as a function of distance between viruses and clays for the experimental conditions (PBS solution: pH 7, IS = 2 mM). The Φ_{dl} values were calculated by eq 7 with Ψ evaluated by eq 3 for the measured zeta potentials and the measured r_v values ($r_v = 80.35$ nm for MS2 and $r_v = 151.3$ nm for ΦX174), and κ evaluated by eq 4 with $T = 298$ K, $N_A = 6.022 \times 10^{23} \text{ mol}^{-1}$, $e = -1.602 \times 10^{-19}$ C, $k_B = 1.381 \times 10^{-23} \text{ J/K}$ and $A_{123} = 7.5 \times 10^{-21}$ J. For the experimental conditions, the repulsive potential is high and the total potential remains positive for long separation distances. Clearly, this suspension is very stable and unfavorable to deposition. Only at the secondary minimum (see Figure 4 insert at $x \sim 70$ nm) MS2 and ΦX174 particles can get closer to clay particles to form clusters. Figure 4 insert emphasizes the magnitude of the calculated secondary energy minima and suggests that MS2 and ΦX174 are weakly

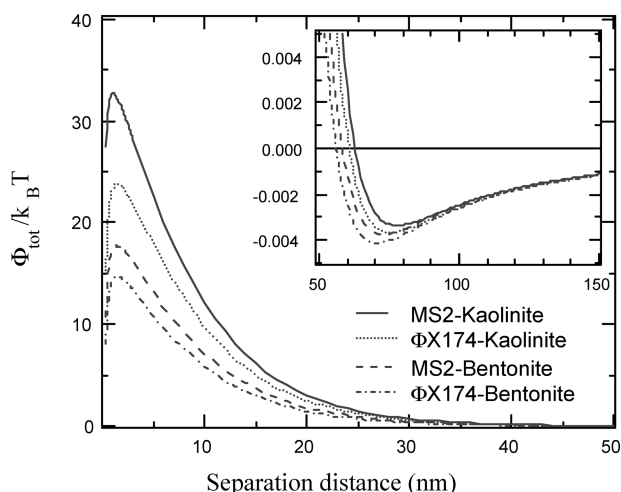


FIGURE 4. Calculated total interaction energy profiles for MS2 and Φ X174 with kaolinite and bentonite as a function of separation distance for the experimental conditions (pH 7, IS = 2 mM). The figure insert highlights the corresponding secondary energy minima.

attached onto both clays. Bacteriophage particles unable to overcome the energy barrier may remain attached onto clays within the secondary energy minimum unless they have sufficient energy to escape (63–65).

Clearly, there exists unfavorable attachment (viruses attach onto clay surfaces in the secondary energy minimum) at pH 7 and IS = 2 mM for MS2 and Φ X174 onto both clays (see Figure 4). The repulsive peaks under the unfavorable conditions are higher for MS2 (32.7 $k_B T$) than Φ X174 (23.4 $k_B T$) for kaolinite. For bentonite, lower energy barriers are observed for both viruses (17.4 $k_B T$ for MS2 and 14.5 $k_B T$ for Φ X174).

Predictions of energy barriers and secondary energy minima are strongly dependent on the model selected for electrostatic double layer interaction calculations. Probably, the constant potential interaction model used in this study does not fully capture the electrostatic double layer interactions between bacteriophages and clays. Interactions between solid surfaces in water can be described well by the DLVO model for most systems at $x \geq 10$ nm. For smaller x values, non-DLVO forces often yield strong interaction forces that can prevent primary well formation when the surfaces have the same charge. Note that viruses are soft particles comprised of a protein coat enclosing nucleic acid, and they are not ideal spherical particles. Therefore, DLVO theory can only predict the qualitative trend of virus deposition onto clays.

Literature Cited

- Bitton, G. Adsorption of viruses onto surfaces in soil and water. *Water Res.* **1975**, *9* (5–6), 473–484.
- Meschke, J. S.; Sobsey, M. D. Comparative adsorption of Norwalk virus, poliovirus 1 and F+ RNA coliphage MS2 to soils suspended in treated wastewater. *Water Sci. Technol.* **1998**, *38* (12), 187–189.
- Babich, H.; Stotzky, G. Reductions in inactivation rates of bacteriophages by clay minerals in lake water. *Water Res.* **1980**, *14*, 185–187.
- Ripp, S.; Miller, R. V. Effect of suspended particulates on the frequency of transduction among *Pseudomonas aeruginosa* in a freshwater environment. *Appl. Environ. Microbiol.* **1995**, *61*, 1214–1219.
- Sim, Y.; Chrysikopoulos, C. V. One-dimensional virus transport in porous media with time dependent inactivation rate coefficients. *Water Resour. Res.* **1996**, *32*, 2607–2611.
- Chrysikopoulos, C. V.; Sim, Y. One-dimensional virus transport in homogeneous porous media with time-dependent distribution coefficient. *J. Hydrol.* **1996**, *185*, 199–219.

- Schiffenbauer, M.; Stotzky, G. Adsorption of coliphages T1 and T7 to clay minerals. *Appl. Environ. Microbiol.* **1982**, *43*, 590–596.
- Lipson, S. M.; Stotzky, G. Adsorption of reovirus to clay minerals: Effects of cation-exchange capacity, cation saturation, and surface area. *Appl. Environ. Microbiol.* **1983**, *46*, 673–682.
- Ryan, J. N.; Harvey, R. W.; Metge, D.; Elimelech, M.; Navigato, T.; Pieper, A. P. Field and laboratory investigations of inactivation of viruses (PRD1 and MS2) attached to iron oxide-coated quartz sand. *Environ. Sci. Technol.* **2002**, *36* (11), 2403–2413.
- Zhuang, J.; Jin, Y. Virus retention and transport as influenced by different forms of soil organic matter. *J. Environ. Qual.* **2003**, *32* (3), 816–823.
- Chattopadhyay, S.; Puls, R. W. Adsorption of bacteriophages on clay minerals. *Environ. Sci. Technol.* **1999**, *33*, 3609–3614.
- Aronino, R.; Dlugy, C.; Arkhangelsky, E.; Shandalov, S.; Oron, G.; Brenner, A.; Gitis, V. Removal of viruses from surface water and secondary effluents by sand filtration. *Water Res.* **2009**, *43*, 87–96.
- Chu, Y.; Jin, Y.; Yates, M. V. Virus transport through saturated sand columns as affected by different buffer solutions. *J. Environ. Qual.* **2000**, *29*, 1103–1110.
- Yuan, B.; Pham, M.; Nguyen, T. H. Deposition kinetics of bacteriophage MS2 on a silica surface coated with natural organic matter in a radial stagnation point flow cell. *Environ. Sci. Technol.* **2008**, *42*, 7628–7633.
- Langlet, J.; Gaboriaud, F.; Duval, J. F. L.; Gantzer, C. Aggregation and surface properties of F-specific RNA phages: implication for membrane filtration processes. *Water Res.* **2008**, *42*, 2769–2777.
- Langlet, J.; Gaboriaud, F.; Gantzer, C. Effects of pH on plaque forming unit counts and aggregation of MS2 bacteriophage. *J. Appl. Microbiol.* **2007**, *103*, 1632–1638.
- Ohshima, H. Electrophoresis of soft particles. *Adv. Colloid Interfac.* **1995**, *62*, 189–235.
- Duval, J. F. L.; Ohshima, H. Electrophoresis of diffuse soft particles. *Langmuir.* **2006**, *22*, 3533–3546.
- Schaldach, C. M.; Bourcier, W. L.; Shaw, H. F.; Viani, B. E.; Wilson, W. D. The influence of ionic strength on the interaction of viruses with charged surfaces under environmental conditions. *J. Colloid Interface Sci.* **2006**, *294*, 1–10.
- van Olphen, H. *An Introduction to Clay Colloid Chemistry*; Interscience: New York, 1963.
- Zhao, H.; Low, P. F.; Bradford, J. M. Effects of pH and electrolyte concentration on particle interaction in three homoionic sodium soil clay suspensions. *Soil Sci.* **1991**, *151*, 196–207.
- Schroth, B. K.; Sposito, G. Surface charge properties of kaolinite. *Clays Clay Miner.* **1997**, *45*, 85–91.
- Gu, Y.; Li, D. The ζ -potential of glass surface in contact with aqueous solutions. *J. Colloid Interface Sci.* **2000**, *226*, 328–339.
- Grundl, T.; Reese, C. Laboratory study of electrokinetic effects in complex natural sediments. *J. Hazard. Materials.* **1997**, *55*, 187–201.
- Loveland, J. P.; Ryan, J. N.; Amy, G. L.; Harvey, R. W. The reversibility of virus attachment to mineral surfaces. *Colloids Surf., A* **1996**, *107*, 205–221.
- Vilker, V. L.; Fong, J. C.; Seyed-Hoseyni, M. Poliovirus adsorption to narrow particle size fractions of sand and montmorillonite clay. *J. Colloid Interface Sci.* **1983**, *92*, 422–435.
- Shields, P. A. Factors influencing virus adsorption to solids. Ph.D. Dissertation, University of Florida, Gainesville, FL, 1986.
- Adams, M. H. *Bacteriophages*; Interscience: New York, N.Y., 1959; pp 450–454.
- Schulze, D. G. *Soil Mineralogy with Environmental Applications*, SSSA Book Series No. 7; Soil Science Society of America: Madison, WI, 2002; Vol. 7.
- Alkan, M.; Karadas, M.; Doğan, M.; Demirbas, O. Electrokinetic properties of kaolinite in mono- and multivalent electrolyte solutions. *Colloid Surf., A* **2005**, *83*, 51–59.
- Thompson, S. S.; Flury, M.; Yates, M. V.; Jury, W. A. Role of the air-water-solid interface in bacteriophage sorption experiments. *Appl. Environ. Microbiol.* **1998**, *64*, 304–309.
- Thompson, S. S.; Yates, M. V. Bacteriophage inactivation at the air-water-solid interface in dynamic batch systems. *Appl. Environ. Microbiol.* **1999**, *65*, 1186–1190.
- Zhao, B.; Zhang, H.; Zhang, J.; Jin, Y. Virus adsorption and inactivation in soil as influenced by autochthonous microorganisms and water content. *Soil Biol. Biochem.* **2008**, *40*, 649–659.
- Jin, Y.; Chu, Y.; Li, Y. Virus removal and transport in saturated and unsaturated sand columns. *J. Contam. Hydrol.* **2000**, *43*, 111–128.

- (35) Chu, Y.; Jin, Y.; Baumann, T.; Yates, M. V. Effect of soil properties on saturated and unsaturated virus transport through columns. *J. Environ. Quality*. **2003**, *32*, 2017–2025.
- (36) Poletika, N. N.; Jury, W. A.; Yates, M. V. Transport of bromide, simazine, and MS-2 coliphage in a lysimeter containing undisturbed, unsaturated soil. *Water Resour. Res.* **1995**, *31*, 801–810.
- (37) Hurst, C. J.; Gerba, C. P.; Cech, I. Effects of Environmental variables and soil characteristics on virus survival in soil. *Appl. Environ. Microbiol.* **1980**, *40*, 1067–1079.
- (38) Gerba, C. P. Applied and theoretical aspects of virus adsorption to surfaces. *Adv. Appl. Microbiol.* **1984**, *30*, 133–168.
- (39) Yates, M. V.; Yates, S. R. Modeling microbial fate in the subsurface environment. *Crit. Rev. Environ. Control.* **1988**, *17* (4), 307–344.
- (40) Sim, Y.; Chrysikopoulos, C. V. Analytical models for one-dimensional virus transport in saturated porous media. *Water Resour. Res.* **1995**, *31* (5), 1429–1437. (Correction) *Water Resour. Res.* **1996**, *32* (5), 1473.
- (41) Sim, Y.; Chrysikopoulos, C. V. Three-dimensional analytical models for virus transport in saturated porous media. *Transp. Porous Media* **1998**, *30* (1), 87–112.
- (42) Giese, R. F.; van Oss, C. J. *Colloid and Surface Properties of Clays and Related Minerals*; Marcel Dekker Inc.: New York, 2002, 119–139.
- (43) van Oss, C. J.; Giese, R. F.; Costanzo, P. M. DLVO and non-DLVO interactions in hectorite. *Clays Clay Miner.* **1990**, *38* (2), 151–159.
- (44) Ruckenstein, E.; Prieve, D. C. Adsorption and desorption of particles and their chromatographic separation. *AIChE J.* **1976**, *22*, 276–283.
- (45) Gregory, J. Approximate expressions for Retarded van der Waals Interaction. *J. Colloid Interface Sci.* **1981**, *83* (1), 138–145.
- (46) Murray, J. P.; Parks, G. A. In *Particulates in Water: Characterization, Fate, Effects and Removal*, Advances in Chemistry Series 189; Kavanaugh, M. C., Leckie, J. O., Eds.; American Chemical Society: Washington, DC, 1978.
- (47) Hogg, R.; Healy, T. W.; Fuerstenau, D. W. Mutual coagulation of colloidal dispersions. *Trans. Faraday Soc.* **1966**, *62*, 1638–1651.
- (48) Frens, G.; Overbeek, J. Th. G. Repeptization and the theory of electrostatic colloids. *J. Colloid Interface Sci.* **1972**, *38*, 376–387.
- (49) Kallay, N.; Bigkup, B.; Tomid, M.; Matijevic, E. Particle adhesion and removal in model systems: X. The effect of electrolytes on particle detachment. *J. Colloid Interface Sci.* **1986**, *114* (2), 357–362.
- (50) Moore, R. S.; Taylor, D. H.; Sturman, L. S.; Reddy, M. M.; Fuhs, G. W. Poliovirus adsorption by 34 minerals and soils. *Appl. Environ. Microbiol.* **1981**, *42*, 963–975.
- (51) Anders, R.; Chrysikopoulos, C. V. Evaluation of the factors controlling the time-dependent inactivation rate coefficients of bacteriophage MS2 and PRD1. *Environ. Sci. Technol.* **2006**, *40* (10), 3237–3242.
- (52) Kauzmann, W. Some factors in the interpretation of protein denaturation. *Adv. Protein Chem.* **1959**, *14*, 1–63.
- (53) Bales, R. C.; Hinkle, S. R.; Kroeger, T. W.; Stocking, K.; Gerba, C. P. Bacteriophage adsorption during transport through porous media: Chemical perturbations and reversibility. *Environ. Sci. Technol.* **1991**, *25*, 2088–2095.
- (54) Schaub, S. A.; Sagik, B. P. Association of enteroviruses with natural and artificially introduced colloidal solids in water and infectivity of solids-associated virions. *Appl. Microbiol.* **1975**, *30*, 212–222.
- (55) Carlson, G. F., Jr.; Woodard, F. E.; Wentworth, D. F.; Sproul, O. J. Virus inactivation on clay particles in natural waters. *J. Water Pollut. Control Fed.* **1968**, *40*, R89–R106.
- (56) Golmohammadi, R.; Valegard, K.; Fridborg, K.; Liljas, L. The refined structure of bacteriophage MS2 at 2.8 Å resolution. *J. Mol. Biol.* **1993**, *234* (3), 620–639.
- (57) Duran, J. D. G.; Ramos-Tejada, M. M.; Arroyo, F. J.; Gonzalez-Caballero, F. Rheological and electrokinetic properties of sodium montmorillonite suspensions. *J. Colloid Interface Sci.* **2000**, *229*, 107–117.
- (58) de Kerchove, A. J.; Elimelech, M. Relevance of electrokinetic theory for 'soft' particles to bacterial cells: Implications for bacterial adhesion. *Langmuir* **2005**, *21*, 6462–6472.
- (59) Sondi, I.; Milat, O.; Pradvic, V. Electrokinetic potentials of clay surfaces modified by polymers. *J. Colloid Interface Sci.* **1997**, *189*, 66–73.
- (60) Penrod, S. L.; Olson, T. M.; Grant, S. B. Deposition kinetic of two viruses in packed beds of quartz granular media. *Langmuir*. **1996**, *12*, 5576–5587.
- (61) Overby, L. R.; Barlow, G. H.; Doi, R. H.; Jacob, M.; Spiegelman, S. Comparison of two serologically distinct ribonucleic acid bacteriophages. I. Properties of the viral particles. *J. Bacteriol.* **1966**, *91* (1), 442–448.
- (62) Dowd, S. E.; Pillai, S. D.; Wang, S.; Corapcioglu, M. Y. Delineating the specific influence of virus isoelectric point and size on virus adsorption and transport through sandy soils. *Appl. Environ. Microbiol.* **1998**, *64* (2), 405–410.
- (63) Redman, J. A.; Walker, S. L.; Elimelech, M. Bacterial adhesion and transport in porous media: Role of the secondary energy minimum. *Environ. Sci. Technol.* **2004**, *38*, 1777–1785.
- (64) Won, J.; Kim, J.-W.; Kang, S.; Choi, H. Transport and adhesion of *Escherichia coli* JM109 in soil aquifer treatment (SAT): One-dimensional column study. *Environ. Monit. Assess.* **2007**, *129*, 9–18.
- (65) Hahn, M. W.; O'Melia, C. R. Deposition and reentrainment of brownian particles in porous media under unfavorable chemical conditions: Some concepts and applications. *Environ. Sci. Technol.* **2004**, *38*, 210–220.

ES100107A